UNIVERSITÀ DEGLI STUDI DI VERONA

DIPARTIMENTO DI MEDICINA

SCUOLA DI DOTTORATO DI

SCIENZE DELLA VITA E DELLA SALUTE

DOTTORATO DI RICERCA IN

SCIENZE BIOMEDICHE CLINICHE E SPERIMENTALI

31°CICLO /ANNO 2015

TITOLO DELLA TESI DI DOTTORATO

LONGITUDINAL FUNCTION OF HEART AND ITS CORRELATION WITH CARDIAC DISEASES

REALIZZATA IN COTUTELA CON L'ILLINOIS UNIVERSITY OF CHICAGO

S.S.D. MED/09

Coordinatore per l'Università di Verona: Prof Giovanni Targher

Tutori: Per l'Università di Verona: Prof Cristiano fava

Per l'Illinois University of Chicago: Prof Afshin Farzaneh-Far

Dottorando: Dott. Simone Romano

Abstract

Background: Left ventricular pump function requires a complex interplay involving myocardial fibers orientated in the longitudinal, oblique and circumferential directions. Long axis dysfunction is an early marker for several pathological states. In fact, assessment of long axis function can provide independent prognostic information in patients with left ventricular dysfunction. Currently, longitudinal systolic function can be evaluated either by cardiac magnetic resonance or echocardiography, using two main techniques: mitral annular plane systolic excursion (MAPSE) and global longitudinal strain (GLS).
The aims of these Cardiac Magnetic Resonance (CMR) studies were therefore:

1. To assess whether lateral MAPSE, as a surrogate for long axis function, is a predictor of major adverse cardiovascular events (MACE).

2. To evaluate the prognostic value of lateral MAPSE in a large multicenter sample of patients with reduced ejection fraction (EF).

3. To evaluate if lateral MAPSE may provide incremental prognostic information in patients with hypertension.

4. To assess whether CMR feature-tracking derived GLS may provide independent prognostic information in patients with cardiomyopathy in a single center and then in a multicenter study.

Methods: Study 1. Patients referred at the Illinois University of Chicago for clinical CMR with both cine and late gate enhancement (LGE) imaging were prospectively enrolled. Patients were followed for the combined primary outcome of MACE: death, non-fatal myocardial infarction, hospitalization for heart failure or unstable angina, and late revascularization (>90 days after CMR).

Study 2, 3, 4. Four geographically diverse universities in the United States participated in these observational, multicenter studies. We enrolled patients that had undergone clinical CMR at the involved Universities with both cine and late gate enhancement (LGE) imaging. Patients were followed for the primary outcome of all-cause mortality using the Social Security Death Index.

Lateral MAPSE was measured in 4 chamber view as the simple linear displacement between end-diastole and end-systole.

Endocardial left ventricular contours were manually traced in all 3 long-axis cine views to derive GLS using the Qstrain feature tracking package.

Results: Study 1. Patients with reduced lateral MAPSE experienced significantly higher incidence of MACE. After adjustment for established clinical risk factors which were univariate predictors, lateral MAPSE remained a significant independent predictor of MACE. Incorporation of lateral MAPSE into this risk model resulted in a net reclassification improvement (NRI).
Study 2. In patients with lower tertiles of lateral MAPSE the risk of death increased significantly. After adjustment for risk factors which were univariate predictors, lateral MAPSE remained a significant independent predictor of death. Addition of lateral MAPSE to this model resulted in significant improvement in model discrimination.
Study 3. In patients with hypertension lateral MAPSE is a significant independent predictor of mortality. By Kaplan-Meier-analysis, the risk-of-death was significantly higher in patients with lateral MAPSE<median (10mm). Lateral MAPSE was associated with an increased risk-of-death after adjustment for clinical and imaging risk factors. Addition of lateral MAPSE in this model resulted in significant-improvement in the C-statistic. Moreover, lateral MAPSE remained independently associated with death amongst the subgroup of patients with preserved EF as well as in those without a history of myocardial infarction.

Study 4. The risk of death increased significantly with decreasing tertiles of GLS. After adjustment for risk factors, which were univariate predictors, GLS remained a significant independent predictor of death. Addition of GLS to this model resulted in significant improvement in the global chi-square and C statistic.

Conclusions: Reduced long axis function assessed either with lateral MAPSE or GLS during routine cine-CMR is an independent predictor of MACE and all-cause mortality in patients with left ventricle (LV) disfunction and in hypertensives

patients incremental to common clinical and imaging risk factors including EF and LGE. Future studies are needed to explore the role of CMR derived lateral MAPSE and GLS in clinical decision making for these patients.

Table of contents

Background

Longitudinal function of heart

Cardiac pumping is the result of the contraction of myocardial fibers organized in different orientations and different layers[1 2] (figure 1), resulting in longitudinal and circumferential shortening and radial thickening of the ventricles[3] (figure 2). Most of left ventricular fibres are arranged circumferentially, particularly in the mid-wall and the base of the ventricle, however longitudinal fibres are found in the subendocardial and subepicardial free wall as well as in the papillary muscles. Longitudinal shortening can be observed as the movement of the base of the ventricles toward the apex in systole[4 5]. Longitudinal function plays a fundamental role in cardiac movement, contributing to ventricular ejection by reducing longitudinal left ventricle cavity size as the mitral annulus is pulled toward the apex, and has been shown to be an important contributor to left ventricular ejection[6].

During early diastole, the potential energy stored during systole creates ventricular suction, critical in facilitating rapid ventricular filling at low pressures in the normal heart[7]. As the mitral annulus springs back to its equilibrium position, it moves around the column of blood passing through the mitral valve, thus aiding ventricular filling. Through this simple mechanism, blood that was in the left atrium finds itself in the ventricle despite remaining stationary with respect to the apex and chest wall. The motion of the annulus towards the apex during ventricular systole has the effect of correspondingly increasing the capacity of the atrium as its floor moves downwards - thus drawing blood into the atrium from the pulmonary veins[6 8]. During atrial systole, atrial emptying and ventricular filling are further facilitated as the mitral annulus is pulled away from the apex by contraction of atrial myocardium, which is inserted into it[9].

Thus, longitudinal movement of the mitral annulus is a major component of normal heart function. Longitudinal annular movement therefore appears to be a dominant contributor to left ventricular pump function in adults. CMR has been used to measure the contribution of long axis function to overall stroke volume in normal

subjects, elite athletes and patients with dilated cardiomyopathy [6]. Several studies have demonstrated that as much as 60% of stroke volume is explained by longitudinal function[10].

Possibly because of their subendocardial location, most of longitudinal myocardial fibers seem to be exquisitely sensitive to disturbance by various pathologies[11].

Mitral annular motion is rapidly affected by ischemia and there is a very close interaction between long axis function and coronary artery disease[12]

Figure 1. Myocardial fibers of heart. Longitudinal fibers are superficial, circumferential are located in the middle myocardium, oblique fibers are in the deep myocardium

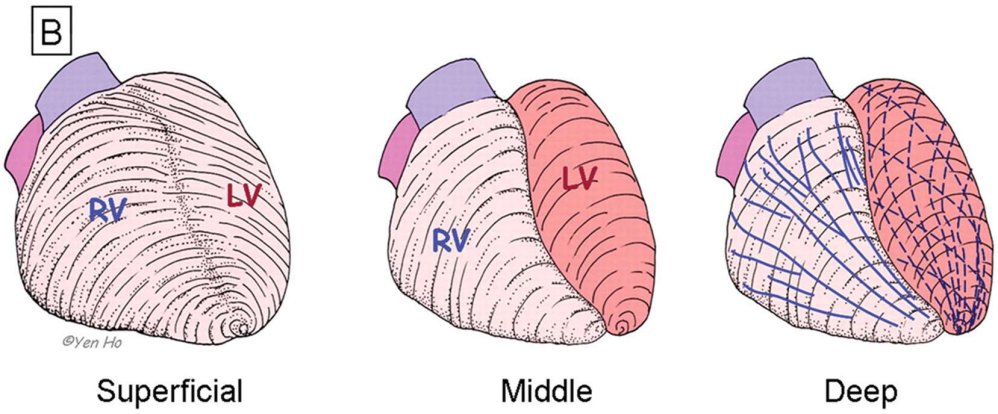

Figure 2. Radial thickening, longitudinal and circumferential shortening of the left ventricle

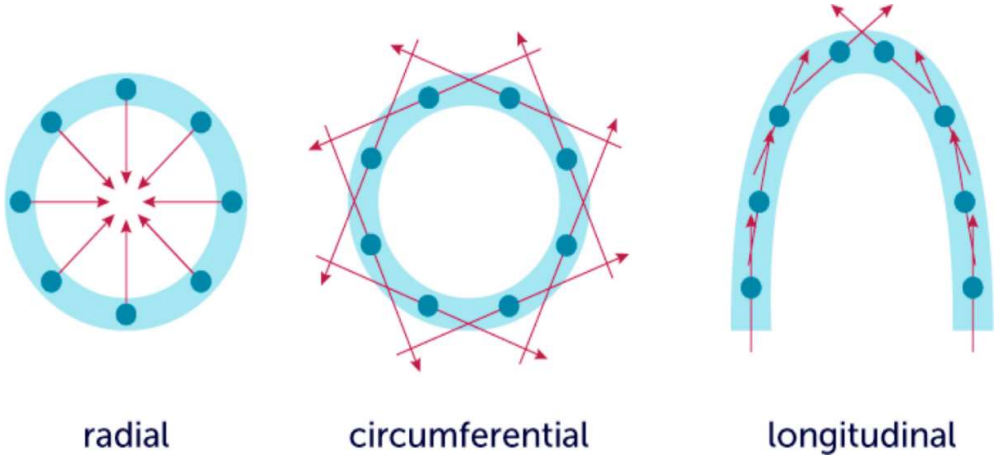

Assessment of left ventricle longitudinal systolic function

Assessment of longitudinal systolic function may overcome most limitations of standard systolic indices and offer detailed additional information, therefore providing a valid integration to classic measures of global and circumferential systolic performance. Currently, longitudinal systolic performance can be evaluated either by cardiac magnetic resonance or by echocardiography, using two main techniques: MAPSE and GLS.

MAPSE

Since the cardiac apex is fixed with respect to the chest wall, changes in long axis function can be assessed by measuring changes in the position of the atrioventricular annulus[11]. Indeed, early studies used M-mode echocardiography to directly follow the position of the mitral annulus and measure MAPSE[13] (figure 3). However, M-mode echocardiographic MAPSE assessment suffers from angle dependence issues.

Measurements are usually performed at the septal and/or lateral annulus level from the apical 4-chamber view, using the zoom function. MAPSE is conventionally measured as the distance between the nadir of the M-mode annular motion profile—corresponding to the maximal backward displacement from left ventricle apex after

the electrocardiographic P wave—and the peak shortening, i.e., the point of maximum upward excursion towards left ventricle apex. Because annular excursion reflects the global performance of left ventricle sub-endocardial longitudinal fibers, MAPSE is currently used as an index of global left ventricle longitudinal systolic function. A lateral MAPSE of 10 mm is commonly used to identify normality [14]. Measurement of MAPSE has the advantage of being simple, highly reproducible, quickly performed, and feasible in nearly all patients even in the presence of suboptimal image quality [15].

Figure 3. Measurement of MAPSE using the M-mode imaging of the lateral mitral annular motion

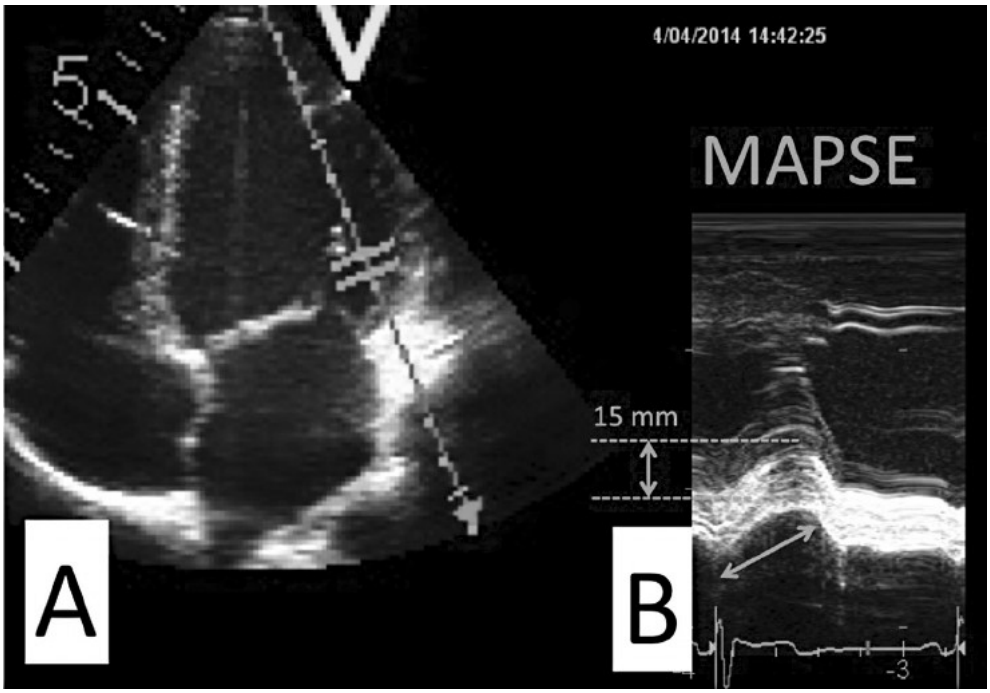

MAPSE can also be measured by CMR in 4-chamber view. Lateral mitral annular positions can be marked at end-diastole, the images is advanced frame-by-frame to end-systole (just before mitral valve opening) where lateral mitral annular position is again identified. Lateral MAPSE is defined as the distance between the lateral mitral annular position at end-diastole to the lateral mitral annular position at end-

systole. Thus, MAPSE is measured as the simple linear displacement between end-diastole and end-systole (Figure 4).

Figure 4. Assessment of lateral MAPSE in 4-chamber cardiac magnetic resonance. Lateral mitral annular positions was recorded at end diastole (left panel, *red dot*) and end systole (right panel, *red line*), allowing for assessment of lateral MAPSE

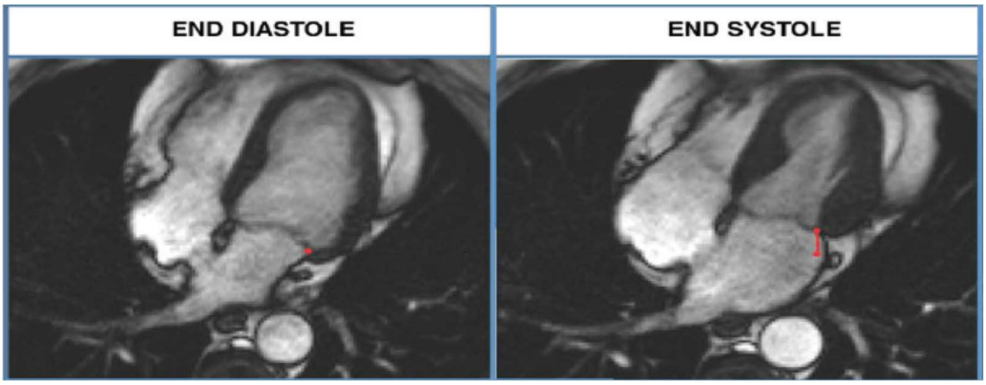

Strain analysis

There are three different types of myocardial deformation (figure 5). The sum of the three different longitudinal strain represents myocardial deformation directed from the base to the apex. During systole, ventricular myocardial fibers shorten with a translational movement from the base to the apex; the consequent reduction of the distance between single kernels is represented by negative trend curves. Through longitudinal strain analyses in 4-chamber, 2-chamber, 3-chamber and apical long-axis views, both regional (relative to each of the 17 LV segments) and global strain values (global longitudinal strain) can be obtained. GLS recently has been validated as a quantitative index for global LV function. Normal reference ranges for GLS have been determined by meta-analysis of study control groups and healthy volunteers. In 24 studies involving 2,597 subjects, normal values ranged from 15.9% to 22.1% (mean 19.7%; 95% CI: 20.4 to 18.9%)[16].The same measurement can be applied to the speckle-tracking echocardiographic analysis of longitudinal myocardial deformation of the left ventricle and right ventricle, obtaining the peak atrial longitudinal strain and the right ventricle longitudinal strain respectively.

Figure 5. Speckle-tracking echocardiographic analysis of myocardial deformation showing measurements of longitudinal strain (upper), radial strain (intermediate), and circumferential strain (lower).

Sergio Mondillo and al. Speckle-Tracking Echocardiography. A New Technique for Assessing Myocardial Function. J Ultrasound Med 2011; 30:71–83

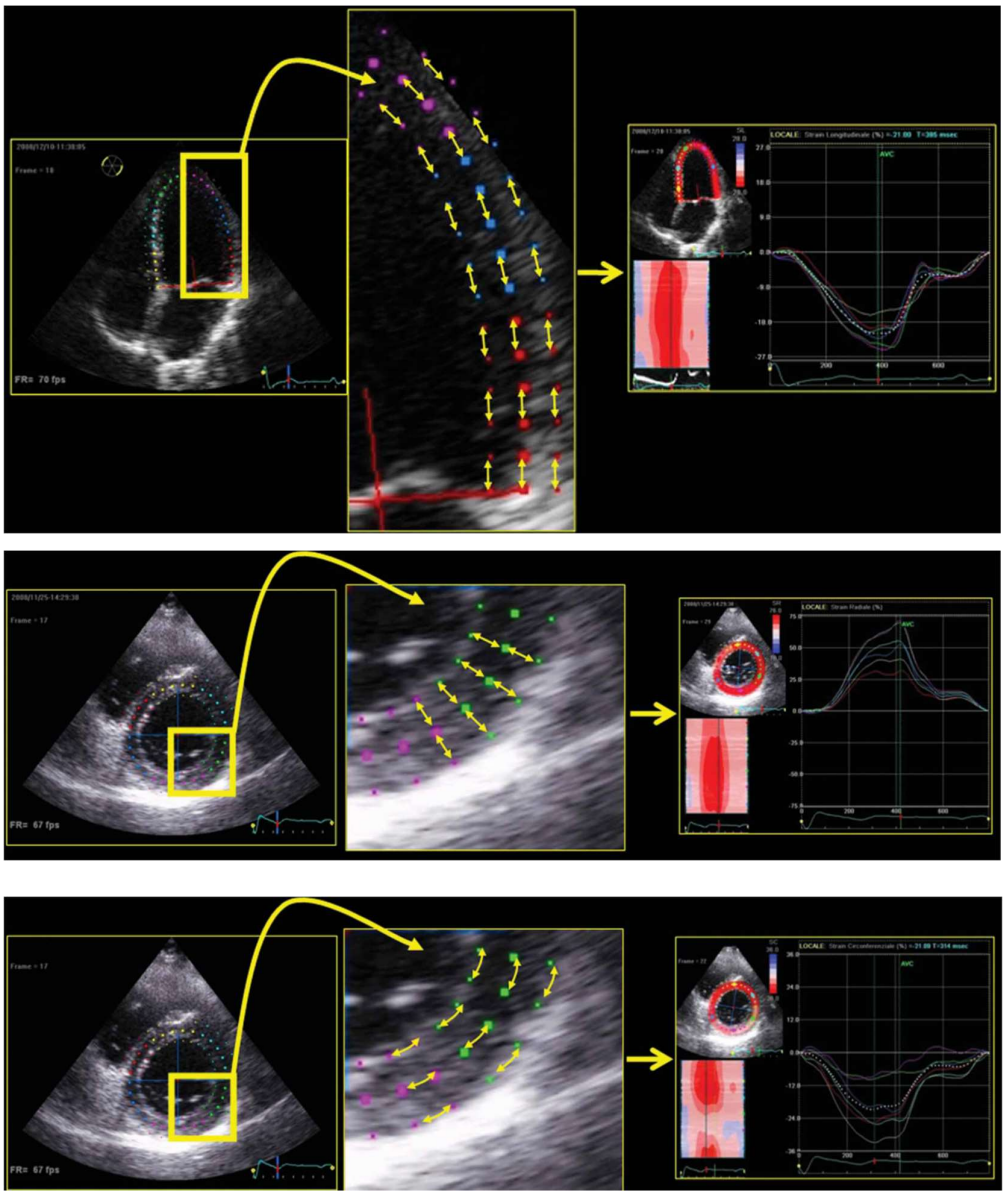

Speckle Tracking 2D Strain

Recently, enormous interest has been generated by development of echocardiographic 2D speckle tracking techniques to assess long axis function in a more global manner by measuring GLS[17 18 19]. The raw ultrasonic signal or radio frequency signal that creates the ultrasonic image consists of numerous random speckles. Any given point on an ultrasonic image can be identified by its unique speckle pattern. Using these speckle patterns (speckle tracking) to identify specific points in the myocardium, strain can be calculated and displayed. Because 2D echo is distance, the initial measurement is strain. There is a variety of ways to demonstrate or present this strain information. By tracking the displacement of speckles during the cardiac cycle, speckle-tracking echocardiography allows semiautomated elaboration of myocardial deformation in 3 spatial directions: longitudinal, radial, and circumferential. In addition, speckle-tracking echocardiography offers an evaluation of the occurrence, direction, and velocity of left ventricle rotation [20]. The semiautomated nature of speckle-tracking echocardiography guarantees good intraobserver and interobserver reproducibility [21].

CMR feature tracking

Recent development of CMR feature tracking technology shows promise in allowing measurement of longitudinal strain using routine cine images in the clinical setting[22]. The underlying principle is based on recognition of 'patterns of features' or 'irregularities' in the image that are tracked and followed in successive images[22].

Importantly, this approach can be applied to routine cine CMR acquisitions thus avoiding the need for dedicated pulse sequences.

Similar to echo speckle tracking, there are inter-vendor differences in the exact algorithms used in CMR feature tracking. Moreover, measurements are not necessarily directly comparable between modalities, or with those based on dedicated CMR pulse sequences. Nevertheless, several recent studies comparing

speckle tracking echo and CMR feature tracking have suggested good agreement[23] [24].

MAPSE and GLS

MAPSE and GLS provide differing measures of left ventricular function. GLS uses specialized software to give a global measure of relative longitudinal change in length by tracking patterns within the myocardium and can also provide segmental information. By contrast, lateral MAPSE is a simple measure of displacement which incorporates primarily basal longitudinal movement and possibly an element of mitral annular radial contraction[25]. It requires no specialized software for its measurement. So far, there has been no analysis of the relative prognostic value of these two parameters. Therefore, the relative prognostic value of speckle tracking derived GLS and MAPSE would be very interesting.

Methods of the studies

In the first study we prospectively enrolled four hundred consecutive outpatients referred at the Illinois University of Chicago for clinical CMR. We excluded patients with metallic implants incompatible with CMR, glomerular filtration < 30 ml/min, severe claustrophobia, or mitral valve replacement. Information on demographic variables and laboratory testing was obtained from patient interviews and the electronic medical record. Patients were followed for the combined primary outcome of MACE: death, non-fatal myocardial infarction, hospitalization for heart failure or unstable angina, and late revascularization (>90 days after CMR). Clinical follow-up was obtained by review of the electronic medical records. The Social Security Death Index was used to confirm all cases of death.

In the second, third and fourth study, four geographically diverse universities in the United States (University of Illinois at Chicago, Duke University, New York Methodist, Houston de Bakey) participated in these observational, multicenter studies, the University of Illinois in Chicago served as the data coordinating center. We used a cloud-based database containing de-identified searchable data from consecutive patients with full DICOM datasets from the participating centers. Baseline demographics were obtained by local site investigators at the time of the clinical study.

We enrolled 1060 patients with an ejection fraction <50% in the second study, 1,735 hypertensives patients in the third study, 1047 patients with an ejection fraction <50% in the fourth study, who had undergone clinical CMR in 2011 at the involved Universities with both cine and late gate enhancement (LGE) imaging. Patients were followed for the primary outcome of all-cause mortality using the Social Security Death Index.

In the single center part of the fourth study, consecutive patients (n=470) undergoing CMR at the Illinois University of Chicago, with both cine and LGE imaging with EF <50%, were included retrospectively. Comprehensive phenotyping, including clinical history, imaging, and cardiac catheterization, classified 330 individuals with ischemic and 140 with non-ischemic cardiomyopathy. Patients were followed for the primary outcome of all-cause

mortality using the US Social Security Death Index.

Statistical analysis

Normally distributed data were expressed as mean ± SD. Continuous variables were compared by the Student's t-test or Wilcoxon rank-sum (depending on data normality). Comparisons of discrete variables were made using the chi-square test; Fisher's exact test was used when the assumptions of the chi-square test were not met. Kaplan-Meier methods (log-rank) were used to evaluate the relationship between lateral MAPSE or GLS and time to the primary outcome of MACE or all-cause mortality. Cox proportional hazards regression modelling was used to identify factors that were independently associated with MACE or all-cause mortality. All models were assessed for collinearity and proportional hazards assumption. For the multivariable model, risk factors which were univariate predictors at $p \leq 0.10$ were considered as candidate variables. To assess the added prognostic value of lateral MAPSE and GLS, the final model was compared with a model in which lateral MAPSE or GLS was not included. The global chi-square statistic was calculated for both models, and compared using the likelihood ratio test. Model discrimination was compared by calculating the C-statistic as well as the integrated discrimination improvement (IDI), which measures the improvement in sensitivity and specificity of the model with addition of the new predictor. Formal risk reclassification analyses were conducted with calculation of continuous net reclassification improvement (NRI) as well as categorical NRI using categories of <10%, 10–20%, and ≥20% mortality to define low, intermediate, and high-risk categories, respectively. A p value of <0.05 was considered statistically significant.

Study 1

MAPSE and MACE

The first part of our research focused on the correlation between MAPSE and MACE. We hypothesized that MAPSE measured during CMR imaging reflects changes in long axis function and may be an early marker for adverse cardiovascular outcomes. The aim of this study was to assess whether MAPSE is a predictor of MACE.

Results

Table 1 summarizes baseline patient characteristics. Median MAPSE for the population was 1.11 cm. Moreover, LVEF was significantly higher in patients with MAPSE ≥ 1.11 cm.

A total of 72 MACE occurred during a median follow-up of 14.5 months. This was comprised of 11 deaths, 10 non-fatal myocardial infarctions, 12 hospitalizations for heart failure, 28 hospitalizations for unstable angina, and 11 late revascularizations. Overall, patients with lateral MAPSE <median had twice the number of cumulative MACE when compared to those with lateral MAPSE ≥ median (24 % vs 12 %, p = 0.0018). By Kaplan-Meier analysis, patients with lateral MAPSE < median experienced significantly higher incidence of MACE than patients with lateral MAPSE ≥ median (log- rank p = 0.027) (Fig. 6).

Table 1 Baseline Characteristics Stratified by Median Level of MAPSE

Characteristics	Total	Lateral MAPSE < median	Lateral MAPSE ≥ median	*P* Value
	N = 400	*N* = 195	*N* = 205	
Age (±SD)	57.9 (±14.7)	59.7 (±14.6)	56.2 (±14.6)	0.017
Male %	44.8	47.7	42.0	0.248
BMI (±SD)	30.6 (±6.4)	31.0 (±6.5)	31.1 (±6.3)	0.876
Diabetes %	32.5	38.5	26.8	0.013
Hyperlipidemia %	52.0	56.9	47.3	0.055
Smoking %	18.0	23.6	12.7	0.005
Hypertension %	73.8	76.4	71.2	0.238
Known CAD %	31.1	36.6	25.9	0.020
Prior MI %	13.3	16.4	10.2	0.069
Prior PCI %	15.8	19.5	12.2	0.045
Prior CABG %	3.8	3.1	4.4	0.490
NYHA class	0.6 (±0.9)	0.5 (±0.9)	0.6 (±1.0)	0.295
Heart Failure %				
None	69.2	70.7	67.8	0.543
NYHA 1	12.1	12.6	11.6	0.760
NYHA 2	12.3	11.5	13.1	0.642
NYHA 3	5.4	4.7	6.0	0.564
NYHA 4	0.5	0.5	0.5	0.977
Antiplatelet Drug %	53.3	52.5	54.1	0.788
Statin %	50.1	49.6	52.1	0.684
ACE inhibitor %	40.4	43.9	40.0	0.235
Beta Blocker %	64.2	64.7	63.7	0.853
Diuretic %	46.5	42.0	50.7	0.144
LVEF (±SD)	58.9 (±13.7)	55.5 (±15.6)	62.2 (±10.7)	<0.001
LV mass g (±SD)	118.8 (±43.3)	123.6 (±48.1)	114.6 (±38.3)	0.039
LGE present %	20.9	26.7	15.3	0.006

ACE angiotensin converting enzyme, *BMI* body mass index, *CABG* coronary artery bypass grafting, *CAD* coronary artery disease, *LGE* late gadolinium enhancement, *LVEF* left ventricular ejection fraction, *MAPSE* Mitral Annular Plane Systolic Excursion, *MI* myocardial infarction, *NYHA class* New York Heart Association Class (class 0 signifies no heart failure), *PCI* percutaneous coronary intervention, *SD* standard deviation

Figure 6. Kaplan Meier curves for MACE in patients with lateral MAPSE above and below the median. The number of patients at risk at each time interval for each group is presented

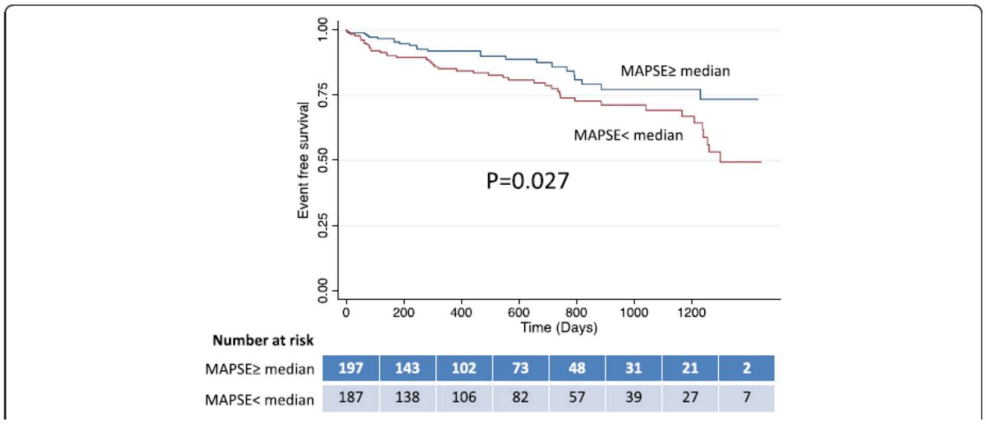

By univariable analysis, age, diabetes, hypertension, NYHA class, LV mass and lateral MAPSE were associated with occurrence of MACE (at $p \leq 0.10$) (Table 2). The highest cumulative incidence of MACE occurred in those with MAPSE < median and LVEF < 55%. In the multivariable analysis after adjustment for established clinical risk factors which were univariate predictors, lateral MAPSE remained a significant independent predictor of MACE (HR = 4.384, 95% CI 1.257-15.271, per cm decrease; p = 0.020) (Table 2). Addition of lateral MAPSE to this model resulted in a significant increase in global chi-square as assessed by the likelihood ratio test (p = 0.03) and an integrated discrimination improvement of 0.01 (p = 0.01). Overall, the net reclassification improvement (NRI) was 0.18 (p = 0.006) across risk categories of MACE.

Table 2 Univariable and multivariable predictors of MACE

Variables	Univariable		Multivariable	
	Hazard Ratio (95 % CI)	*P* Value	Hazard Ratio (95 % CI)	*P* Value
Age	1.016 (0.999–1.033)	0.0585	0.985 (0.958–1.013)	0.286
Male	1.014 (0.638–1.612)	0.9531	-	-
Diabetes	1.693 (1.058–2.713)	0.0309	0.863 (0.428–1.740)	0.680
Hyperlipidemia	1.326 (0.825–2.131)	0.2397	-	-
Smoking	0.998 (0.555–1.795)	0.9953	-	-
Hypertension	2.482 (1.189–5.181)	0.0066	2.355 (0.820–6.766)	0.112
NYHA class	0.810 (0.618–1.060)	0.1080	0.853 (0.519–1.403)	0.532
LVEF	1.001 (0.985–1.017)	0.9234	-	-
LGE present	1.263 (0.757–2.110)	0.3794	-	-
LV mass	1.009 (1.002–1.017)	0.0211	1.008 (1.000–1.015)	0.044
Lateral MAPSE[a]	2.228 (1.051–4.679)	0.0331	4.384 (1.257–15.271)	0.020
Septal MAPSE[a]	1.585 (0.682–3.715)	0.2865	-	-

LGE late gadolinium enhancement, *LV* left ventricular, *LVEF* left ventricular ejection fraction, *MAPSE* Mitral Annular Plane Systolic Excursion, *NYHA* New York Hear Association. [a]per cm decrease

Study 2

MAPSE and mortality in patients with reduced EF

At this stage, we wanted to evaluate the prognostic value of lateral MAPSE in a large multicenter population of patients with reduced ejection fraction undergoing CMR at several centers in the United States.

Results

Table 3 summarizes baseline patient characteristics. Mean lateral MAPSE for the population was 9.1mm. Median lateral MAPSE was 9.0mm (interquartile range: 7.8-10.0 mm).

A total of 132 deaths occurred during a median follow-up of 4.4 years (interquartile range: 3.6-5.1 years).

Table 3. Baseline Characteristics stratified by tertiles of lateral MAPSE. ACE = angiotensin converting enzyme, ARB = angiotensin receptor blocker, BMI = body mass index, LVEDV = LV end diastolic volume index, LVEF = LVEF, LVESV = LV end systolic volume index.

***Except where indicated, data are numbers of patients, with percentages in parentheses.**

†Data are means ± standard deviations.

Characteristics	All Patients ($n = 1040$)*	Lateral MAPSE <7.8 mm ($n = 346$)*	Lateral MAPSE 7.8–10.0 mm ($n = 345$)*	Lateral MAPSE >10.0 mm ($n = 349$)*	*P* Value
Mean age (y)†	59.5 ± 15.8	62.1 ± 16.2	60.1 ± 14.7	56.5 ± 16.0	<.001
Male (%)	676 (65.0)	227 (65.7)	209 (60.5)	238 (68.2)	.123
Mean BMI (kg/m²)†	28.7 ± 8.5	28.7 ± 11.6	29.0 ± 6.5	28.5 ± 6.3	.700
Diabetes (%)	320 (30.8)	108 (31.2)	120 (34.9)	93 (26.8)	.071
Hyperlipidemia (%)	560 (53.9)	179 (51.7)	198 (57.5)	185 (52.9)	.282
Smoking (%)	149 (14.3)	48 (14.0)	44 (12.8)	56 (16.0)	.490
Hypertension (%)	695 (66.8)	239 (69.0)	248 (72.0)	210 (60.2)	.002
Aspirin (%)	653 (62.8)	219 (63.3)	242 (70.1)	194 (55.7)	.001
Statin (%)	575 (55.3)	181 (52.4)	206 (59.7)	188 (54.0)	.158
ACE inhibitor or ARB (%)	692 (66.6)	223 (64.4)	294 (70.7)	208 (59.7)	.077
Beta blocker (%)	513 (49.3)	181 (52.2)	133 (54.5)	146 (42.0)	.003
Diuretic (%)	466 (44.8)	186 (53.9)	163 (47.4)	119 (34.1)	<.001
LVEDV index (mL/m²)†	117.4 ± 52.9	122.6 ± 60.6	119.4 ± 51.7	110.7 ± 45.0	.008
LVESV index (mL/m²)†	66.3 ± 43.7	77.9 ± 53.1.8	68.0 ± 40.0	54.0 ± 32.9	<.001
LV mass index (g/m²)†	113.8 ± 28.3	114.1 ± 41.0	110.2 ± 42.2	116.9 ± 45.1	.853
LGE present (%)	645 (62.0)	232 (67.2)	206 (59.7)	204 (58.4)	.043
LVEF (%)†	33.8 ± 10.0	29.4 ± 10.4	33.7 ± 9.4	38.0 ± 8.2	<.001

By Kaplan-Meier analysis, the risk of death increased significantly with decreasing tertiles of lateral MAPSE (log-rank p=0.0001) (Figure 7). Kaplan-Meier analysis of patients with EF≤35% vs. those with EF>35% stratified by the highest and lowest tertiles of lateral MAPSE shows that mortality was significantly higher in patients with lower lateral MAPSE, irrespective of EF (Figure 8).

Figure 7. Kaplan Meier curves of lateral MAPSE stratified by tertiles of lateral MAPSE

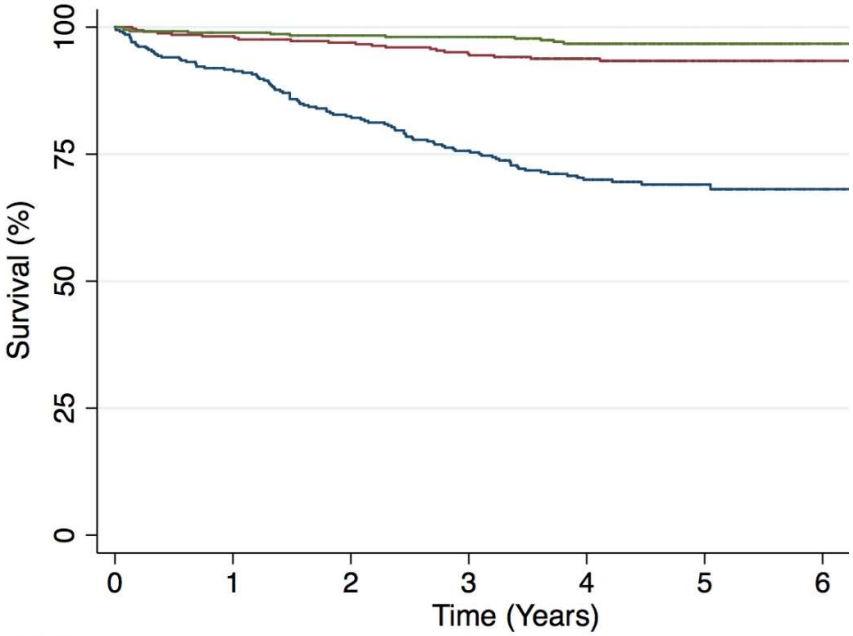

Number at risk							
tertile = 0	338	301	267	242	179	79	12
tertile = 1	331	321	311	303	231	98	9
tertile = 2	367	357	345	338	248	118	22

Figure 8. Kaplan Meier curves stratified by ejection fraction

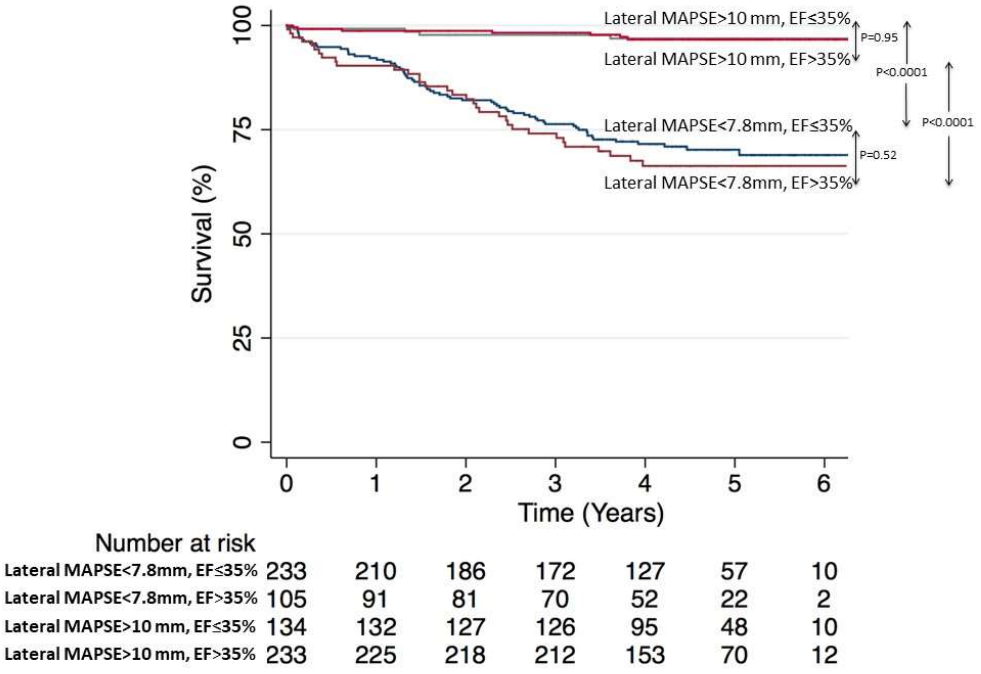

After adjustment for risk factors which were univariate predictors at p≤0.15 (age, body mass index, diabetes, LV end-diastolic volume index, LGE, EF), lateral MAPSE remained a significant independent predictor of death (HR=1.724, 95% CI, 1.571-1.892, per mm decrease; p<0.001) (Table 4). Addition of lateral MAPSE to this model resulted in a significant increase in global chi-square as assessed by the likelihood ratio test (global chi-square increased from 50.54 to 203.94; p<0.0001) and an integrated discrimination improvement of 0.192 (95% CI 0.133, 0.258). Moreover, addition of lateral MAPSE resulted in significant improvement in model discrimination as assessed by the C statistic (C statistic increased from 0.675 to 0.844 p<0.0001).

Overall, the categorical net reclassification improvement (NRI) was 0.507 (95% CI, 0.312-0.684); 0.279 (95% CI, 0.147-0.450) for patients with events, and 0.228 (95% CI 0.120-0.300) for patients without events. Continuous NRI was 1.036 (95% CI, 0.878-1.194).

Table 4. Multivariable model of mortality. BMI=Body Mass Index, CI=Confidence Interval, LGE=Late Gadolinium Enhancement, LVEDV =Left Ventricular End Diastolic Volume Index, LVEF=Left Ventricular Ejection Fraction, MAPSE=Mitral Annular Plane Systolic Excursion. * per mm decrease.

VARIABLES	Multivariable	
	Hazard Ratio (95% CI)	P Value
Age	**1.019 (1.007-1.032)**	**0.003**
BMI	**1.012 (1.001-1.023)**	**0.032**
Diabetes	**1.588 (1.110-2.272)**	**0.011**
LVEDV index	1.000 (0.996-1.005)	0.857
Lateral MAPSE *	**1.724 (1.571-1.892)**	**<0.001**
LGE present	**1.916 (1.254-2.929)**	**0.003**
LVEF	1.023 (0.992-1.048)	0.057

Study 3

MAPSE and mortality in patients with hypertension

We then, given the known adverse consequences of myocardial involvement in hypertension, hypothesized that CMR-derived lateral MAPSE may provide incremental prognostic information in these patients. In patients with hypertension, the heart is a major target of end organ damage. Moreover, cardiac abnormalities including left ventricular hypertrophy and dysfunction have been shown to be powerful predictors of adverse outcomes in these individuals[26]. As a consequence, echocardiographic evaluation of myocardial structure and function is commonly used in the risk assessment of patients with hypertension[27].

Results

Table 5 summarizes baseline patient characteristics stratified by lateral MAPSE above and below the median (10mm).

Table 5. baseline patient characteristics stratified by lateral MAPSE above and below the median (10mm)

CHARACTERISTICS	Total	MAPSE <10mm	MAPSE ≥10mm	P Value
Age (±SD), years	62.6 (±13.2)	64.5 (±13.1)	60.9 (±13.1)	<0.001
Male %	57.5	59.3	55.9	0.180
BMI (±SD), kg/m2	30.0 (±8.8)	29.7 (±10.6)	30.4 (±6.6)	0.073
Diabetes %	34.5	37.7	31.5	0.007
Hyperlipidemia %	64.2	66.2	62.3	0.088
Smoking %	11.4	13.3	9.8	0.023
History of MI %	21.6	25.8	18.1	<0.001
Aspirin %	62.0	67.0	57.3	<0.001
Statin %	57.3	59.9	54.9	0.038
ACE inhibitor or ARB %	50.2	55.8	44.9	<0.001
Beta Blocker %	39.0	45.2	33.2	<0.001
Diuretic %	43.6	49.5	38.0	<0.001
Heart Rate (±SD), beats/min	73.4 (±15.0)	77.3 (±15.7)	69.7 (±13.2)	<0.001
Systolic BP (±SD), mmHg	131.7(±21.2)	129.0(±21.1)	134.2(±21.1)	<0.001
Diastolic BP (±SD), mmHg	75.0(±13.3)	75.4(±13.6)	74.5(±13.1)	0.210
LVEDV index (±SD), ml/m2	75.5 (±31.7)	83.1 (±35.4)	68.2 (±25.8)	<0.001
LVESV index (±SD), ml/m2	39.4 (±30.1)	50.6 (±33.8)	28.7 (±21.3)	<0.001
LV mass index (±SD), g/m2	97.4 (±39.8)	105.4 (±42.2)	89.9 (±35.9)	<0.001
LGE present %	42.7	55.6	30.5	<0.001
LGE extent (±SD), %	5.1 (±8.7)	7.1 (±9.8)	3.3 (±6.9)	<0.001
LVEF (±SD), %	49.3 (±17.4)	41.2 (±17.0)	57.0 (±13.9)	<0.001

Of the 1,735 patients in this study, 235 died during a median follow-up of 5.1years (interquartile range: 3.4-6.1 years).

When stratified by the median value of lateral MAPSE (10mm), Kaplan-Meier analysis showed significantly increased risk of death in those with lateral MAPSE<median (log-rank p<0.0001) (Figure 9).

Figure 9. Kaplan Meier curves of lateral MAPSE stratified by the median value of lateral MAPSE (10mm)

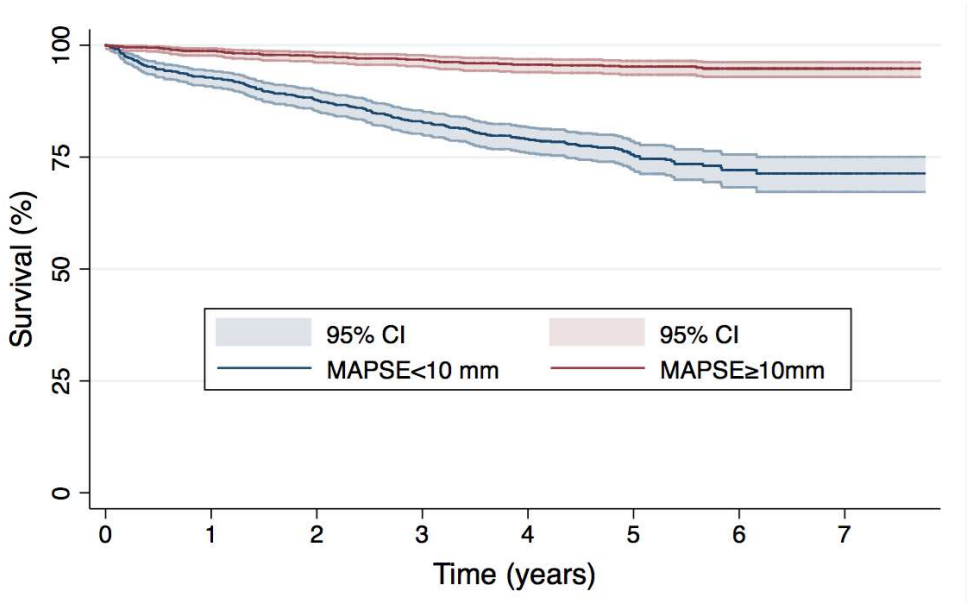

After adjustment for clinical and imaging risk factors, which were univariate predictors at p≤0.10 (age, gender, diabetes, history of MI, ACE or ARB use, diuretic use, heart rate, systolic BP, diastolic BP, LV end-diastolic volume index, LV end-systolic volume index, LV mass index, LGE, EF), lateral MAPSE remained a significant independent predictor of death (HR=1.402, 95% CI 1.323-1.486, per mm decrease; p<0.001) i.e. each 1mm worsening in lateral MAPSE was associated with an 40.2% increase risk of death (Table 6). Addition of lateral MAPSE into the model with clinical and imaging predictors resulted in significant increase in the C-statistic (from 0.735 to 0.815 p<0.0001) and an integrated. GLS was also measured, it remained a significant predictor of events in the final multivariable model. Thus, both lateral MAPSE and GLS were independently associated with death in this

population. Moreover, there was no evidence of problematic strong collinearity between GLS and lateral MAPSE (variance inflation factor was 1.37).

Table 6. Uni and multivariable model of mortality with lateral MAPSE adjusted to univariate clinical and imaging predictors (at p≤0.10) for the whole population. ACE=Angiotensin Converting Enzyme, ARB=Angiotensin Receptor Blocker, BMI=Body Mass Index, LGE=Late Gadolinium Enhancement, LVEDV =Left Ventricular End Diastolic Volume Index, LVEF=Left Ventricular Ejection Fraction, LVESV =Left Ventricular End Systolic Volume Index, MAPSE=Mitral Annular Plane Systolic Excursion, MI=Myocardial Infarction, SD=standard deviation. * per mm decrease. ‡ per % decrease.

VARIABLES	Univariable		Multivariable	
	Hazard Ratio (95% CI)	**P Value**	**Hazard Ratio (95% CI)**	**P Value**
Age	**1.034 (1.023-1.045)**	**<0.001**	**1.021 (1.010-1.033)**	**<0.001**
Male	**1.413 (1.073-1.859)**	**0.014**	-	-
BMI	0.983 (0.963-1.003)	0.095	-	-
Diabetes	**1.372 (1.057-1.781)**	**0.018**	-	-
Hyperlipidemia	1.074 (0.819-1.409)	0.606	-	-
Smoking	1.176 (0.786-1.758)	0.430	-	-
History of MI	**1.394 (1.043-1.863)**	**0.025**	-	-
Aspirin	1.194 (0.907-1.571)	0.205	-	-
Statin	0.972 (0.746-1.267)	0.833	-	-
ACE inhibitor or ARB	0.673 (0.429-1.055)	0.084	-	-
Beta Blocker	1.006 (0.762-1.327)	0.968	-	-
Diuretic	**1.472 (1.132-1.913)**	**0.004**	-	-
Heart Rate	**1.023 (1.016-1.031)**	**<0.001**	**1.013 (1.004-1.021)**	**0.004**
Systolic BP	**0.992 (0.985-0.998)**	**0.009**	-	-

Diastolic BP	**0.984 (0.974-0.994)**	**0.002**	**0.983 (0.973-0.993)**	**0.001**
LVEDV index	**1.006 (1.002-1.010)**	**0.001**	-	-
LVESV index	**1.008 (1.005-1.012)**	**<0.001**	-	-
LV mass index	**1.004 (1.001-1.007)**	**0.005**	-	-
LGE	**2.701 (2.061-3.541)**	**<0.001**	**1.622 (1.211-2.174)**	**0.001**
Lateral MAPSE*	**1.477 (1.403-1.555)**	**<0.001**	**1.402 (1.323-1.486)**	**<0.001**
GLS	**1.210 (1.180-1.240)**	**<0.001**	**1.180 (1.137–1.224)**	**<0.001**
LVEF ‡	**1.024 (1.016-1.031)**	**<0.001**	-	-

Seventy-seven deaths occurred amongst the 896 patients with preserved EF (≥50%). When stratified by the median value of lateral MAPSE (12mm), Kaplan-Meier analysis showed significantly increased risk of death in those with lateral MAPSE<median (log-rank p<0.0001) (Figure 10). Each 1mm decrease in lateral MAPSE was associated with a 33.9% increase risk-of-death after adjustment for clinical and imaging risk factors (HR=1.339; p<0.001) (Table 7). GLS remained a significant predictor of events in the final multivariable model (HR: 1.210; $p < 0.001$). Thus, both MAPSE and GLS were independently associated with death in this subpopulation.

Figure 10. Kaplan Meier curves in patients with preserved ejection fraction stratified by the median value of lateral MAPSE (12mm).

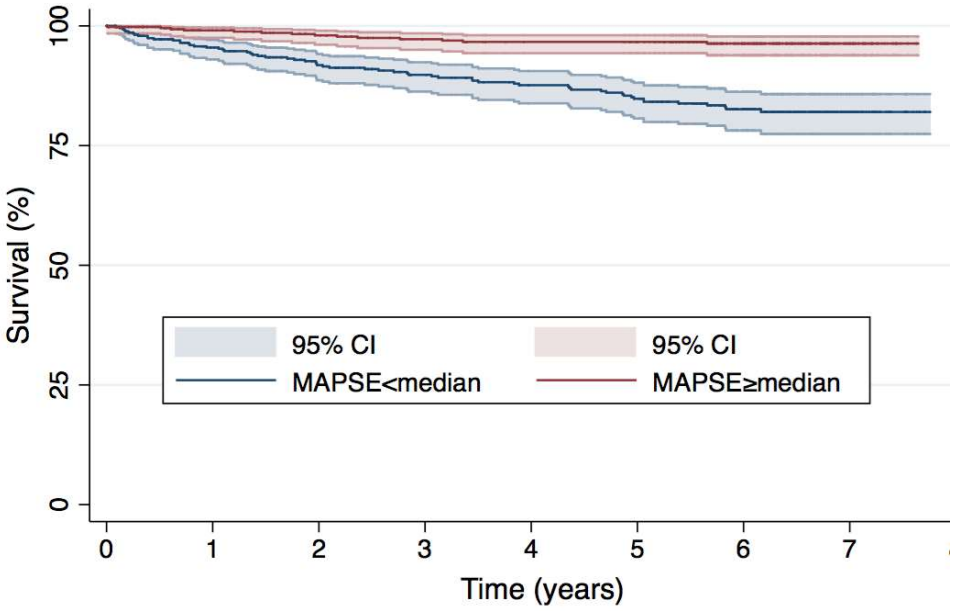

Table 7. Multivariable model of mortality with lateral MAPSE adjusted to univariate clinical and imaging predictors (at p≤0.10) for patients with preserved ejection fraction. ACE=Angiotensin Converting Enzyme, ARB=Angiotensin Receptor Blocker, BMI=Body Mass Index, LGE=Late Gadolinium Enhancement, LVEDV =Left Ventricular End Diastolic Volume Index, LVEF=Left Ventricular Ejection Fraction, LVESV =Left Ventricular End Systolic Volume Index, MAPSE=Mitral Annular Plane Systolic Excursion, MI=Myocardial Infarction, SD=standard deviation. * per mm decrease. ‡ per % decrease.

VARIABLES	Univariable		Multivariable	
	Hazard Ratio (95% CI)	P Value	Hazard Ratio (95% CI)	P Value
Age	**1.049 (1.028-1.071)**	**<0.001**	**1.040 (1.018-1.064)**	**<0.001**
Male	1.548 (0.959-2.500)	0.070	-	-
BMI	**0.948 (0.912-0.985)**	**0.004**	**0.955 (0.917-0.994)**	**0.025**
Diabetes	1.378 (0.865-2.197)	0.185	-	-
Hyperlipidemia	0.932 (0.593-1.463)	0.758	-	-
Smoking	0.571 (0.180-1.812)	0.299	-	-
History of MI	0.897 (0.390-2.066)	0.796	-	-
Aspirin	1.010 (0.644-1.584)	0.966	-	-
Statin	1.078 (0.685-1.696)	0.745	-	-
ACE inhibitor or ARB	0.960 (0.604-1.523)	0.859	-	-
Beta Blocker	0.855 (0.499-1.465)	0.563	-	-
Diuretic	1.497 (0.948-2.362)	0.087	-	-
Heart Rate	**1.025 (1.011-1.040)**	**<0.001**	**1.025 (1.010-1.040)**	**0.001**
Systolic BP	1.001 (0.990-1.012)	0.828	-	-
Diastolic BP	0.991 (0.973-1.009)	0.308	-	-
LVEDV index	0.993 (0.980-1.005)	0.250	-	-
LVESV index	1.001 (0.981-1.022)	0.916	-	-

LV mass index	**1.002 (1.001-1.003)**	**0.025**	**1.008 (1.001-1.015)**	**0.020**
LGE	**1.955 (1.214-3.151)**	**0.008**	-	-
Lateral MAPSE*	**1.417 (1.300-1.545)**	**<0.001**	**1.339 (1.224-1.465)**	**<0.001**
GLS	**1.269 (1.211-1.330)**	**<0.001**	**1.210 (1.147-1.277)**	**<0.001**
LVEF ‡	**1.035 (1.000-1.071)**	**0.046**	-	-

One hundred and seventy-two deaths occurred amongst the 1,360 patients without history of myocardial infarction. When stratified by the median value of lateral MAPSE (10.4mm), Kaplan-Meier analysis showed significantly increased risk of death in those with lateral MAPSE<10.4 mm (log-rank p<0.0001) (Figure 11). Each 1mm decrease in lateral MAPSE was associated with a 39.0% increase risk-of-death after adjustment for clinical and imaging risk factors (HR=1.390; p<0.001) (Table 8). GLS remained a significant predictor of events in the final multivariable model (HR: 1.159; p < 0.001). Thus, both MAPSE and GLS were independently associated with death in this subpopulation.

Figure 11. Kaplan Meier curves in patients history of myocardial infarction stratified by the median value of lateral MAPSE (10.4mm).

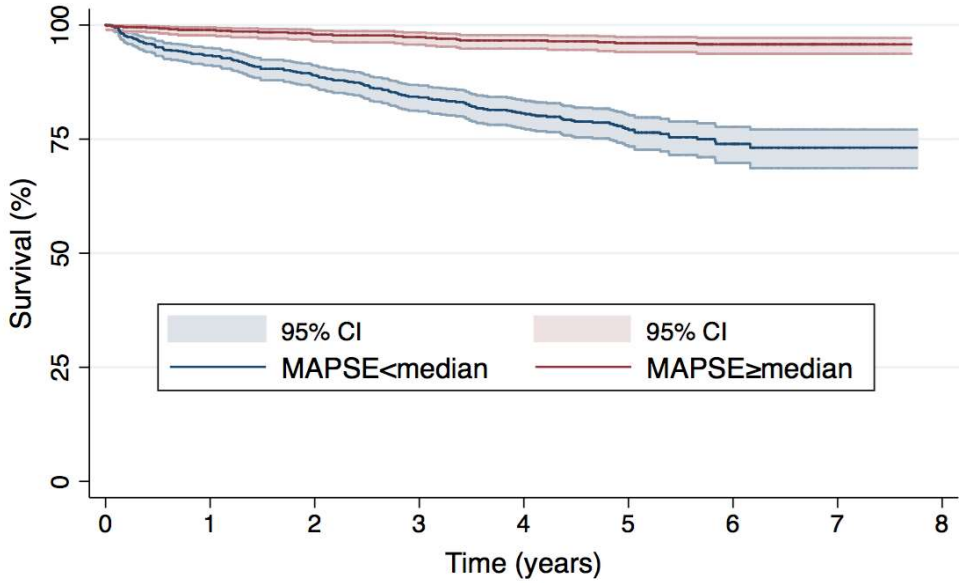

Table 8. Multivariable model of mortality with lateral MAPSE adjusted to univariate clinical and imaging predictors (at p≤0.10) for patients without history of myocardial infarction. ACE=Angiotensin Converting Enzyme, ARB=Angiotensin Receptor Blocker, BMI=Body Mass Index, LGE=Late Gadolinium Enhancement, LVEDV =Left Ventricular End Diastolic Volume Index, LVEF=Left Ventricular Ejection Fraction, LVESV =Left Ventricular End Systolic Volume Index, MAPSE=Mitral Annular Plane Systolic Excursion, MI=Myocardial Infarction, SD=standard deviation. * per mm decrease. ‡ per % decrease.

VARIABLES	Univariable		Multivariable	
	Hazard Ratio (95% CI)	**P Value**	**Hazard Ratio (95% CI)**	**P Value**
Age	**1.040 (1.027-1.053)**	**<0.001**	**1.026 (1.013-1.039)**	**<0.001**
Male	1.467 (0.903-2.385)	0.118	-	-
BMI	**0.961 (0.937-0.986)**	**0.002**	-	-
Diabetes	**1.453 (1.070-1.972)**	**0.018**	-	-
Hyperlipidemia	1.138 (0.836-1.550)	0.409	-	-
Smoking	1.283 (0.766-2.148)	0.360	-	-
Aspirin	1.159 (0.851-1.578)	0.347	-	-
Statin	1.054 (0.776-1.431)	0.738	-	-
ACE inhibitor or ARB	1.123 (0.828-1.522)	0.457	-	-
Beta Blocker	1.099 (0.793-1.522)	0.572	-	-
Diuretic	**1.520 (1.118-2.066)**	**0.008**	-	-
Heart Rate	**1.022 (1.013-1.031)**	**<0.001**	**1.012 (1.002-1.022)**	**0.018**
Systolic BP	0.995 (0.987-1.002)	0.166	-	-
Diastolic BP	**0.985 (0.973-0.996)**	**0.009**	**0.982 (0.971-0.994)**	**0.002**
LVEDV index	1.004 (1.000-1.009)	0.070	-	-
LVESV index	**1.007 (1.003-1.012)**	**0.002**	-	-
LV mass index	**1.004 (1.001-1.007)**	**0.021**	-	-

LGE	**2.960 (2.187-4.006)**	**<0.001**	**1.721 (1.236-2.397)**	**0.001**
Lateral MAPSE*	**1.477 (1.393-1.567)**	**<0.001**	**1.390 (1.299-1.486)**	**<0.001**
GLS	**1.211 (1.178-1.245)**	**<0.001**	**1.159 (1.112-1.207)**	**<0.001**
LVEF ‡	**1.022 (1.031-1.071)**	**<0.001**	-	-

Study 4

GLS and mortality in patients with reduced EF

The single center study

The aim of this study was to evaluate the prognostic-value of CMR feature-tracking derived GLS in a single center-population of patients undergoing evaluation for ischemic or non-ischemic dilated cardiomyopathy.

Results

The mean age of the study population was 60±15years. Sixty-nine percent were male and 30% had diabetes mellitus. The mean EF was 34.2±9.8%. Mean GLS was –10.4±4.6%. Median GLS was –10.3% (interquartile range, –7.1 to –13.6%). During a median follow-up of 4.1years (interquartile range, 3.5–4.8 years), 93(19.8%) patients died. By Kaplan-Meier analysis, the risk of death increased significantly with worsening tertiles of GLS (log-rank P<0.0001) (figure 12).

Figure 12. Kaplan Meier curves of GLS stratified by tertiles of GLS

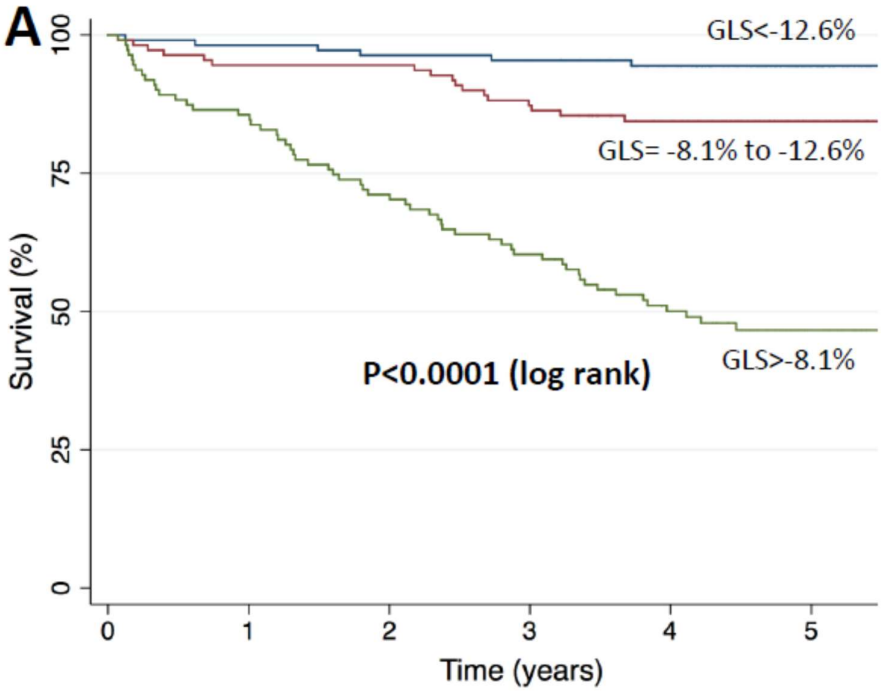

After adjustment for clinical and imaging characteristics (age, body mass index, diabetes mellitus, hypertension, etiology of cardiomyopathy, left ventricular end diastolic volume index, LGE size, EF), which had univariable associations with death (at P≤0.20), GLS remained significantly associated with death (HR, 2.35 per %; 95% CI, 1.81–3.06; P<0.001). In this model, EF remained significantly associated with death (HR, 0.95 per %; 95% CI, 0.91–0.99; P=0.038) but LGE size was not (HR, 1.02 per %; 95% CI, 0.99–1.04; P=0.186). Addition of GLS in this model resulted in significant improvement in the global $\chi 2$ (31–157; P < 0.0001) and C-statistic (0.64–0.85; P<0.0001). Continuous net reclassification improvement was 1.16 (95% CI, 0.95–1.38), with an integrated discrimination improvement of 0.32 (95% CI, 0.22–0.40).

The multicentre study

We then extended this study to a large multicenter population of patients with cardiomyopathy undergoing CMR at several centers in the United States.

Results

Table 9 summarizes baseline patient characteristics.

Table 9. Baseline Characteristics. ACE=Angiotensin Converting Enzyme, ARB=Angiotensin Receptor Blocker, BMI=Body Mass Index, GLS=Global Longitudinal Strain, LGE=Late Gadolinium Enhancement, LVEDV =Left Ventricular End Diastolic Volume Index, LVEF=Left Ventricular Ejection Fraction, LVESV =Left Ventricular End Systolic Volume Index, MI=Myocardial Infarction, SD=standard deviation.

	Total	GLS <−13.0%	GLS −8.7 to −13.0%	GLS >−8.7%	p Value
Age, yrs	59.8 ± 15.7	56.3 ± 16.6	60.2 ± 14.7	62.8 ± 15.1	<0.001
Male	65.3	66.7	62.5	66.9	0.427
BMI, kg/m^2	28.9 ± 8.6	28.2 ± 6.5	28.9 ± 6.6	29.4 ± 11.6	0.199
Diabetes	30.6	24.9	30.2	36.7	0.004
Hyperlipidemia	54.7	50.2	54.9	58.8	0.078
Smoking	14.8	12.9	13.1	18.3	0.085
Hypertension	66.7	61.1	66.8	72.2	0.010
History of MI	28.9	26.1	25.4	35.1	0.010
Ischemic CM	49.9	43.8	43.7	62.1	<0.001
Nonischemic dilated CM	50.1	56.2	56.3	37.9	<0.001
Aspirin	63.2	57.1	60.3	72.3	0.001
Statin	55.9	53.5	56.4	57.8	0.544
ACE Inhibitor or ARB	66.2	57.0	70.5	70.0	0.001
Beta-blocker	49.6	40.8	54.3	53.4	0.001
Diuretic	44.6	31.8	48.8	53.0	0.001
Heart rate, beats/min	76.5 ± 16.5	70.4 ± 13.8	77.5 ± 16.3	81.3 ± 17.4	<0.001
Systolic BP, mm Hg	123.1 ± 20.7	124.9 ± 20.8	124.7 ± 20.6	119.9 ± 20.3	0.010
Diastolic BP, mm Hg	72.7 ± 13.5	72.0 ± 12.9	73.7 ± 13.3	72.4 ± 14.3	0.371
LVEDV index, ml/m^2	117.9 ± 54.6	102.3 ± 40.6	116.7 ± 55.9	134.5 ± 60.3	<0.001
LVESV index, ml/m^2	67.1 ± 44.2	48.7 ± 26.8	67.1 ± 42.2	85.2 ± 51.9	<0.001
LV mass index, g/m^2	113.7 ± 26.4	110.6 ± 27.0	112.9 ± 52.1	117.5 ± 45.1	0.850
LGE present	62.1	51.7	59.5	74.9	<0.001
LGE extent, %	8.4 ± 10.1	6.3 ± 8.4	7.4 ± 9.3	11.6 ± 11.6	<0.001
LVEF, %	33.7 ± 10.0	40.3 ± 6.8	34.0 ± 8.6	26.8 ± 9.3	<0.001

Of the 1012 patients in the study, 133 died during a median follow-up of 4.4 years (interquartile range: 3.6-5.1 years).

By Kaplan-Meier analysis, the risk of death increased significantly with worsening tertiles of GLS (log-rank p<0.0001) (Figure 13).

Figure 13. Kaplan Meier curves of GLS stratified by tertiles of GLS

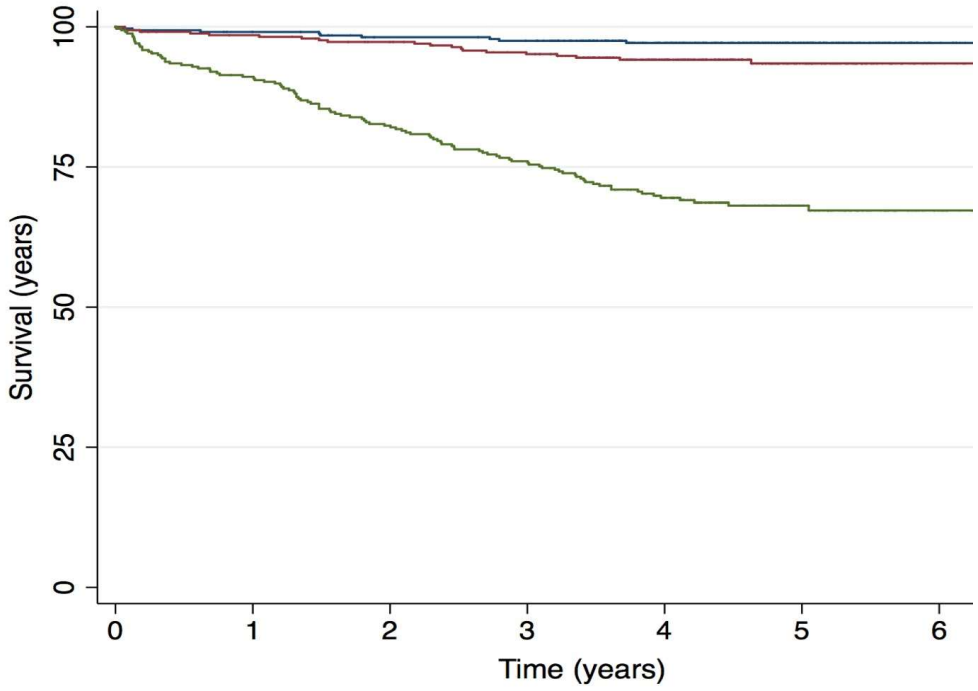

After adjustment for risk factors, which were univariate predictors at p≤0.20 (age, body mass index, diabetes, hyperlipidemia, LV end-diastolic volume index, LGE, EF), GLS remained a significant independent predictor of death (HR=1.888 per percentage decrease p<0.001) (Table 10). Addition of GLS in this model resulted in a significant increase in global Chi-square as assessed by the likelihood ratio test (increasing from 43.14 to 238.33; p<0.0001) and an integrated discrimination improvement of 0.261 (95% CI, 0.196-0.332) with a continuous NRI of 1.215 (95% CI, 1.023-1.333). Moreover, addition of GLS resulted in significant improvement in model discrimination as assessed by the C-statistic (increased from 0.668 to 0.848 p<0.0001). Finally, model global Chi-square and C-statistics showed significant and incremental increase when imaging markers were added to clinical variables in a hierarchical manner (Figure 14).

Table 10. Multivariable model of mortality. BMI=Body Mass Index, CI=Confidence Interval, GLS=Global Longitudinal Strain, LGE=Late Gadolinium Enhancement, LVEDV =Left Ventricular End Diastolic Volume Index, LVEF=Left Ventricular Ejection Fraction.

VARIABLES	Multivariable	
	Hazard Ratio (95% CI)	P Value
Age	**1.016 (1.005-1.027)**	**0.046**
BMI	1.000 (0.990-1.009)	0.925
Diabetes	**1.556 (1.066-2.271)**	**0.022**
Hyperlipidemia	0.732 (0.493-1.087)	0.122
LVEDV index	0.999 (0.995-1.002)	0.559
GLS	**1.888 (1.546-2.305)**	**<0.001**
LGE present	1.327 (0.684-2.038)	0.197
LVEF	1.005 (0.969-1.042)	0.787

Figure 14. Chi square and C-statistics showed significant and incremental increase when imaging markers were added to clinical variables

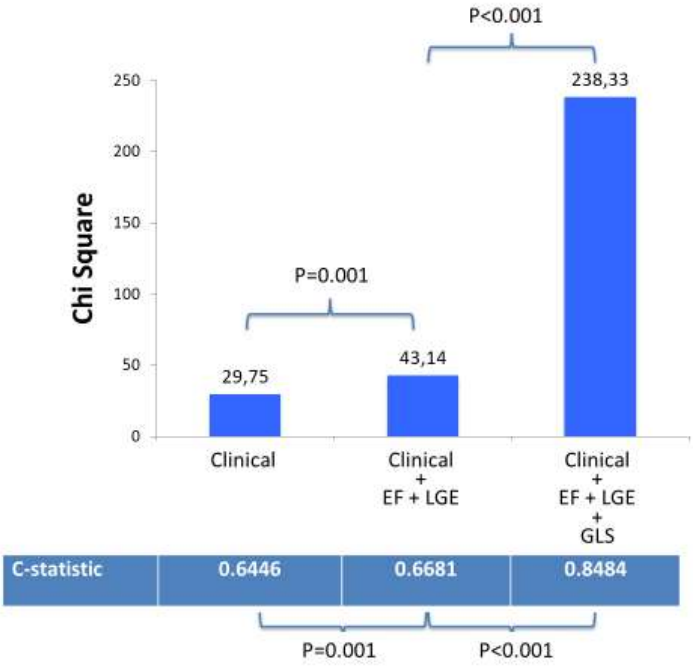

Discussion

MAPSE

MAPSE - as a surrogate for LV long axis function - is a powerful independent predictor of morbidity and mortality. Moreover, we have demonstrated that it provides prognostic information additional to common clinical and imaging risk factors including EF and LGE. Measurements of lateral MAPSE can be obtained from standard cine CMR images without the need for propriety software. These findings may have implications for management decisions based on risk stratification of patients with cardiomyopathy and LV dysfunction. How this information will impact clinical care requires further study. However, it is interesting to note that we found that patients with relatively preserved lateral MAPSE (>10mm) had very few adverse events regardless of whether their EF was above or below 35%. Given that current guidelines recommend ICD placement based primarily on an EF≤35%, it will be interesting to examine the role of long-axis function on sudden cardiac death in future studies.

MAPSE measured using echocardiography has been shown to be a predictor of adverse cardiovascular outcomes in a number of conditions including myocardial infarct, heart failure, atrial fibrillation[28] [29] [30] [31]. However, M-mode MAPSE assessment suffers from angle dependence issues, which were overcome when using CMR as in this study.

Riffel and colleagues showed similar findings using a surrogate CMR measure of long-axis strain derived from the movement of the mitral annulus relative to the apex[32]. Their study patients (n=146) were individuals with non-ischemic cardiomyopathy and EF ≤45 % who were followed for a median of 4.3 years for a composite primary outcome of cardiac death, heart transplantation or aborted sudden cardiac death. Gjesdal et al. examined the prognostic value of similarly derived CMR long axis function from 1,651 individuals in the MESA cohort who were free of cardiovascular disease[33].

In patients with hypertension, the heart is a major target of damage. Moreover, cardiac abnormalities including left ventricular hypertrophy and dysfunction have been shown to be powerful predictors of adverse outcomes in these individuals[34 35]. As a consequence, echocardiographic evaluation of myocardial structure and function is commonly used in the risk assessment of patients with hypertension.

Prior echocardiographic studies have shown that MAPSE is significantly reduced in hypertensive patients even if ejection fraction is preserved[36 37]. In a small single center study, Ballo et al. examined the prognostic value of MAPSE in 156 patients with hypertension and preserved ejection fraction[38]. Over a mean follow-up of 23 months, 24 patients suffered a composite endpoint of heart failure hospitalization, new-onset angina, nonfatal myocardial infarction, coronary revascularization, transient ischemic attack, stroke, and cardiovascular death. Moreover, MAPSE was found to be an independent predictor of the composite endpoint.

The precise mechanism underlying the association between impaired lateral MAPSE and adverse outcomes is unclear. It has been suggested that the subendocardial myocardial fibers (which are more longitudinally aligned) are extremely sensitive to diseases because of greater compressive forces and higher oxygen consumption[11 39 40 41].

The subendocardial fibers are therefore more vulnerable to increased wall stress and imbalances between oxygen supply and demand which may be seen in early stages of hypertension. Interestingly, in an animal model of hypertension, longitudinal function was shown to progressively deteriorate with time compared to control animals and was associated with histological subendocardial fibrosis[42]

GLS

GLS, measured by feature tracking CMR, is a powerful independent predictor of mortality, in a large multicenter population of patients with cardiomyopathy.

There is now a large body of literature demonstrating the diagnostic and prognostic utility of GLS in various cardiovascular disorders[43 44 45]. Even in rare disease such as amyloidosis a reduction of GLS has been demonstrated[46]. Another recent study[47] was designed to show the diagnostic importance of two-dimensional speckle-tracking imaging in differentiating cardiac amyloidosis from other causes of LV hypertrophy; the authors found that the amyloid heart is characterized by reduced basal strain and regional variations in LS from base to apex with a relative 'apical sparing'.

However, these echo strain techniques are highly dependent on attainment of good quality imaging and there is lack of standardization between different vendors[18]. Moreover, suboptimal acoustic windows, apical foreshortening and far field drop out may result in time-consuming analysis requiring significant operator experience[19].

There is a significant and growing body of literature demonstrating the prognostic value GLS derived using speckle tracking echo in patients with cardiomyopathy[17 43 48 49].

In contrast, data regarding CMR derived GLS and prognosis has been very limited so far. Buss and colleagues recently demonstrated that feature tracking derived GLS was an independent predictor of the composite endpoint of cardiac death, heart transplantation, and aborted sudden cardiac death in a small population of 210 dilated cardiomyopathy patients followed for a median of 5.3 years[50]. Our findings are consistent with these prior studies in suggesting that after adjustment for GLS, LVEF is not a significant predicator of events. This study builds on prior data by demonstrating the independent and incremental prognostic value of CMR feature tracking GLS in a multicenter cardiomyopathy population - with a significantly greater number of patients and hard events. These findings greatly expand the evidence base for CMR derived GLS and prognosis.

Head-to-head comparison between MAPSE and GLS

To the best of our knowledge, there has been no analysis of the relative prognostic value of these 2 parameters. The hypertension study has shown that both CMR-derived lateral MAPSE and feature tracking GLS are independently associated with death in patients with hypertension and provide complimentary prognostic information. Lateral MAPSE provides incremental prognostic information to clinical and imaging variables including GLS. Conversely, GLS provides incremental prognostic information to clinical and imaging variables including lateral MAPSE. Given intermodality and intervendor differences in GLS acquisition methods, these findings are not necessarily applicable to echocardiography. Therefore, the relative prognostic values of speckle tracking-derived GLS and echo-derived MAPSE require further study both in hypertension and in other conditions.

Role of CMR in cardiomyopathies

CMR has evolved into a major tool for diagnosis and prognostic assessment of patients with cardiomyopathy by providing data on morphology, function, perfusion, viability and tissue characterization[51 52 53 54 55]. It is the reference standard for measurement of ventricular volumes, mass, and function, allowing serial assessment of disease progression or treatment response in individual patients51 52 54 55. CMR tissue characterization can help establish the underlying cause of a cardiomyopathy51 52 54 55. The presence and extent of LGE allows assessment of the likelihood of recovery of function after revascularization, medical therapy or cardiac resynchronization51 52 54 55. LGE is a powerful predictor of adverse cardiovascular outcome in wide range of cardiomyopathies51 52 54 55. In this study we have shown that GLS provides independent prognostic information in patients with cardiomyopathy undergoing CMR. Moreover, this was incremental to standard clinical and CMR variables including LGE and EF. How this information will impact clinical care requires further study. However, it is interesting to note that we found that patients with relatively preserved GLS had very few adverse events

regardless of whether their EF was above or below 35% or whether LGE was present or not. Given that current guidelines recommend ICD placement based primarily on an EF≤35%, it will be interesting to examine the role of GLS on sudden cardiac death in future studies.

Role of CMR in Hypertension

Echocardiography has a well-established role for assessment of cardiac end organ damage and prognosis in hypertension[56 57]. However, CMR is the gold standard for measurement of ventricular volumes, function and mass; and for myocardial tissue characterization with detection of myocardial fibrosis. As such it may play a role in assessment of some patients with hypertension and hypertensive heart disease[58 59]. It also allows identification of diseases that may mimic hypertensive LVH[60]. The presence of focal myocardial fibrosis as detected by LGE is a powerful predictor of adverse cardiovascular outcomes in numerous conditions including hypertension[61 62]. Krittayaphong et al. showed that LGE is a powerful and independent predictor of cardiac death or myocardial infarction in a population of 1644 patients with hypertension followed for a mean of 29 months[63]. Likewise, LGE was a significant independent predictor of death in our patient cohort. Given the co-existence of coronary artery disease, LGE maybe seen in a subendocardial pattern as well as in a more patchy non-coronary mid-myocardial distribution58 [64 65]. Our study suggests that CMR can provide significant incremental prognostic information in patients with hypertension using lateral MAPSE as a marker of longitudinal function. Moreover, measurements of lateral MAPSE can be obtained from conventional cine CMR images without the need for specialized pulse sequences, propriety software, or additional imaging time. Better identification of high-risk hypertensive patients may allow closer follow-up and more directed therapies to be applied. How this information will affect clinical care requires further investigation and future studies are warranted to explore the role of CMR derived lateral MAPSE in clinical decision making. These studies will need to demonstrate that imaging driven patient management improves specific outcomes before such an approach could be

advocated.

Conclusions

We have shown that reduced long axis function assessed with lateral MAPSE during routine cine-CMR is an independent predictor of MACE and is a powerful independent predictor of mortality in patients with left ventricular dysfunction incremental to common clinical and imaging risk factors including EF and LGE.
Even in patients with hypertension, MAPSE measured during routine cine-CMR is a significant independent predictor of mortality incremental to common clinical and imaging risk factors including EF, LV mass and LGE. A major strength of these findings is that they were made in a big multicenter group of hypertensive patients and patients with cardiomyopathy with a large number of hard events which greatly increases the robustness of our results.

GLS measured during routine cine-CMR is a powerful independent predictor of mortality in patients with cardiomyopathy, incremental to common clinical and imaging risk factors including EF and LGE.

Our findings highlight the role of long-axis function in individuals with hypertension and with cardiomyopathy and suggest that consideration may be given to measurement of lateral MAPSE and GLS in these patients. Future studies are needed to explore the role of CMR derived lateral MAPSE and GLS in clinical decision making for these patients.

Bibliography

[1] Rushmer RF, Crystal DK and Wagner C. The functional anatomy of ventricular contraction. Circ Res 1: 162–170, 1953

[2] Greenbaum RA, Gibson DG. Regional non-uniformity of left ventricular wall movement in man. Br Heart J 45: 29 –34, 1981.

[3] McDonald IG. The shape and movements of the human left ventricle during systole. A study by cineangiography and by cineradiography of epicardial markers. Am J Cardiol 26: 221–230, 1970.

[4] Hamilton WF, Rompf JH. Movement of the base of the ventricle and the relative constancy of the cardiac volume. Am J Physiol 102: 559–565, 1932.

[5] Holmgren BS. The movement of the mitro-aortic ring recorded simultaneously by cineroentgenography and electrocardiography. Acta Radiol 27: 171–176, 1946.

[6] Carlsson M, Ugander M, Heiberg E, Arheden H. The quantitative relationship between longitudinal and radial function in left, right, and total heart pumping in humans. Am J Physiol Heart Circ Physiol 2007;293(1):H636–H644.

[7] Riordan MM, Kovacs SJ. Relationship of pulmonary vein flow to left ventricular short-axis epicardial displacement in diastole: model-based prediction with in vivo validation. Am J Physiol Heart Circ Physiol. 2006; 291(3):H1210–5.

[8] Keren G, Sonnenblick EH, LeJemtel TH. Mitral anulus motion. Relation to pulmonary venous and transmitral flows in normal subjects and in patients with dilated cardiomyopathy. Circulation. 1988;78(3):621–9.

[9] Wang K, Ho SY, Gibson DG, Anderson RH. Architecture of atrial musculature in humans. Br Heart J. 1995;73(6):559–65.

[10] Carlsson M, Ugander M, Mosén H, Buhre T, Arheden H. Atrioventricular plane dis placement is the major contributor to left ventricular pumping in healthy adults, athletes, and patients with dilated cardiomyopathy. Am J Physiol Heart Circ Physiol 2007;292(3):H1452–H1459.

[11] Henein MY, Gibson DG. Long axis function in disease. Heart 1999;81:229–31.

[12] Sanderson JE. Left and right ventricular long-axis function and prognosis. Heart. 2008;94(3):262–3.

[13] Zaky A, Grabhorn L, Feigenbaum H. Movement of the mitral ring: a study in ultrasoundcardiography. Cardiovasc Res. 1967;1(2):121–31.

[14]Alam M, Ho¨glund C, Thorstrand C, Hellekant C (1992) Haemodynamicsignificance of the atrioventricular plane displacement in patients with coronary artery disease. Eur Heart J 13:194–200

[15]Yuda S, Inaba Y, Fujii S, Kokubu N, Yoshioka T, Sakurai S, Nishizato K, Fujii N, Hashimoto A, Uno K, Nakata T, Tsuchihashi K, Miura T, Ura N, Natori H, Shimamoto K (2006) Assessment of left ventricular ejection fraction using long-axis systolic function is independent of image quality: a study of tissue Doppler imaging and m-mode echocardiography. Echocardiography 23:846–852. doi:10.1111/j.1540-8175.2006.00331.x

[16] Yingchoncharoen T., Agarwal S., Popović Z.B., and Marwick T.H.: Normal ranges of left ventricular strain: a meta-analysis. J Am Soc Echocardiogr 2013; 26: pp. 185-191

[17] Kalam K, Otahal P and Marwick TH. Prognostic implications of global LV dysfunction: a systematic review and meta-analysis of global longitudinal strain and ejection fraction. Heart. 2014;100:1673-80.

[18] Shah AM and Solomon SD. Myocardial deformation imaging: current status and future directions. Circulation. 2012;125:e244-8.

[19] Pedrizzetti G, Claus P, Kilner PJ and Nagel E. Principles of cardiovascular magnetic resonance feature tracking and echocardiographic speckle tracking for informed clinical

use. Journal of cardiovascular magnetic resonance : official journal of the Society for Cardiovascular Magnetic Resonance. 2016;18:51.

[20]Teske AJ, De Boeck BW, Melman PG, Sieswerda GT, Doevendans PA, Cramer MJ. Echocardiographic quantification of myocardial function using tissue deformation imaging, a guide to image acquisition and analysis using tissue Doppler and speckle tracking. Cardiovasc Ultrasound2007; 5:27.

[21]Van Dalen BM, Soliman OI, Vletter WB, et al. Feasibility and reproducibility of left ventricular rotation parameters measured by speckle tracking echocardiography. Eur J Echocardiogr2009; 10:669–676.

[22] Schuster A, Hor KN, Kowallick JT, Beerbaum P and Kutty S. Cardiovascular Magnetic Resonance Myocardial Feature Tracking: Concepts and Clinical Applications. Circ Cardiovasc Imaging. 2016;9:e004077.

[23] Amaki M, Savino J, Ain DL, Sanz J, Pedrizzetti G, Kulkarni H, Narula J and Sengupta PP. Diagnostic concordance of echocardiography and cardiac magnetic resonance-based tissue tracking for differentiating constrictive pericarditis from restrictive cardiomyopathy. Circ Cardiovasc Imaging. 2014;7:819-27.

[24] Kempny A, Fernandez-Jimenez R, Orwat S, Schuler P, Bunck AC, Maintz D, Baumgartner H and Diller GP. Quantification of biventricular myocardial function using cardiac magnetic resonance feature tracking, endocardial border delineation and echocardiographic speckle tracking in patients with repaired tetralogy of Fallot and healthy controls. Journal of cardiovascular magnetic resonance : official journal of the Society for Cardiovascular Magnetic Resonance. 2012;14:32.

[25] Levack MM, Jassar AS, Shang EK et al. Three-dimensional echocardiographic analysis of mitral annular dynamics: implication for annuloplasty selection. Circulation 2012;126:S183-8.

[26] Levy D, Garrison RJ, Savage DD, Kannel WB, Castelli WP. Prognostic implications of echocardiographically
determined left ventricular mass in the Framingham Heart Study. The New England

journal of medicine 1990;322:1561-6.

[27] Marwick TH, Gillebert TC, Aurigemma G et al. Recommendations on the use of echocardiography in adult hypertension: a report from the European Association of Cardiovascular Imaging (EACVI) and the American Society of Echocardiography (ASE)dagger. European heart journal cardiovascular Imaging 2015;16:577-605

[28] Diller GP, Kempny A, Liodakis E, Alonso-Gonzalez R, Inuzuka R, Uebing A, Orwat S, Dimopoulos K, Swan L, Li W et al. Left ventricular longitudinal function predicts life-threatening ventricular arrhythmia and death in adults with repaired tetralogy of fallot. Circulation. 2012;125(20):2440–6.

[29] Brand B, Rydberg E, Ericsson G, Gudmundsson P, Willenheimer R. Prognostication and risk stratification by assessment of left atrioventricular plane displacement in patients with myocardial infarction. Int J Cardiol. 2002;83(1):35–41.

[30] Rydberg E, Arlbrandt M, Gudmundsson P, Erhardt L, Willenheimer R. Left atrioventricular plane displacement predicts cardiac mortality in patients with chronic atrial fibrillation. Int J Cardiol. 2003;91(1):1–7.

[31] Willenheimer R, Cline C, Erhardt L, Israelsson B. Left ventricular atrioventricular plane displacement: an echocardiographic technique for rapid assessment of prognosis in heart failure. Heart. 1997;78(3):230–6.

[32] Riffel JH, Keller MG, Rost F, Arenja N, Andre F, Aus dem Siepen F, Fritz T, Ehlermann P, Taeger T, Frankenstein L, Meder B, Katus HA and Buss SJ. Left ventricular long axis strain: a new prognosticator in non-ischemic dilated cardiomyopathy? Journal of cardiovascular magnetic resonance : official journal of the Society for Cardiovascular Magnetic Resonance. 2016;18:36.

[33] Gjesdal O, Yoneyama K, Mewton N, Wu C, Gomes AS, Hundley G, Prince M, Shea S, Liu K, Bluemke DA and Lima JA. Reduced long axis strain is associated with heart failure and cardiovascular events in the multi-ethnic study of Atherosclerosis. J Magn Reson Imaging. 2016;44:178-85.

[34] Levy D, Garrison RJ, Savage DD, Kannel WB, Castelli WP. Prognostic implications of echocardiographically determined left ventricular mass in the Framingham Heart Study. The New England journal of medicine 1990;322:1561-6.

[35] Marwick TH, Gillebert TC, Aurigemma G et al. Recommendations on the use of echocardiography in adult hypertension: a report from the European Association of Cardiovascular Imaging (EACVI) and the American Society of Echocardiography (ASE)dagger. European heart journal cardiovascular Imaging 2015;16:577-605.

[36] Xiao HB, Kaleem S, McCarthy C, Rosen SD. Abnormal regional left ventricular mechanics in treated hypertensive patients with 'normal left ventricular function'. International journal of cardiology 2006;112:316-21.

[37] Ballo P, Quatrini I, Giacomin E, Motto A, Mondillo S. Circumferential versus longitudinal systolic function in patients with hypertension: a nonlinear relation. Journal of the American Society of Echocardiography : official publication of the American Society of Echocardiography 2007;20:298-306.

[38] Ballo P, Barone D, Bocelli A, Motto A, Mondillo S. Left ventricular longitudinal systolic dysfunction is an independent marker of cardiovascular risk in patients with hypertension. American journal of hypertension 2008;21:1047-54.

[39] Henein MY, Gibson DG. Normal long axis function. Heart 1999;81:111-3.

[40] Hu K, Liu D, Herrmann S et al. Clinical implication of mitral annular plane systolic excursion for patients with cardiovascular disease. European heart journal cardiovascular Imaging 2013;14:205-12.

[41] Chilian WM. Microvascular pressures and resistances in the left ventricular subepicardium and subendocardium. Circulation research 1991;69:561-70.

[42] Ishizu T, Seo Y, Kameda Y et al. Left ventricular strain and transmural distribution of structural remodeling in hypertensive heart disease. Hypertension 2014;63:500-6.

[43] Romano S, Mansour IN, Kansal M, Gheith H, Dowdy Z, Dickens CA, Buto-Colletti C, Chae JM, Saleh HH, Stamos TD. Left Ventricular global longitudinal strain predicts heart failure readmission in acute decompensated heart failure. Cardiovasc Ultrasound. 2017 Mar 15;15(1):6. doi: 10.1186/s12947-017-0098-3.

[44] Mignot A, Donal E, Zaroui A, et al: Global longitudinal strain as a major predictor of cardiac events in patients with depressed left ventricular function: A multicenter study. J Am SocEchocardiogr 2010;23:1019–1024.

[45] Tony Stanton, MBChB, PhD; Rodel Leano, BS et al: Prediction of All-Cause Mortality From Global Longitudinal Speckle Strain. Comparison with ejection fraction and wall motion scoring. CircCardiovasc Imaging. 2009;2:356-364.)

[46] Buss S.J., Emami M., Mereles D., et al: Longitudinal left ventricular function for prediction of survival in systemic light-chain amyloidosis: incremental value compared with clinical and biochemical markers. J Am Coll Cardiol 2012; 60: pp. 1067-1076

[47] Phelan D., Collier P., Thavendiranathan P., et al: Relative apical sparing of longitudinal strain using two-dimensional speckle-tracking echocardiography is both sensitive and specific for the diagnosis of cardiac amyloidosis. Heart 2012; 98: pp. 1442-1448

[48] Bertini M, Ng AC, Antoni ML, Nucifora G, Ewe SH, Auger D, Marsan NA, Schalij MJ, Bax JJ and Delgado V. Global longitudinal strain predicts long-term survival in patients with chronic ischemic cardiomyopathy. Circ Cardiovasc Imaging. 2012;5:383-91.

[49] Stanton T, Leano R and Marwick TH. Prediction of all-cause mortality from global longitudinal speckle strain: comparison with ejection fraction and wall motion scoring. Circ Cardiovasc Imaging. 2009;2:356-64.

[50] Buss SJ, Breuninger K, Lehrke S, Voss A, Galuschky C, Lossnitzer D, Andre F, Ehlermann P, Franke J, Taeger T, Frankenstein L, Steen H, Meder B, Giannitsis E, Katus HA and Korosoglou G. Assessment of myocardial deformation with cardiac magnetic resonance strain imaging improves risk stratification in patients with dilated cardiomyopathy. European heart journal cardiovascular Imaging. 2015;16:307-15.

51 Karamitsos TD, Francis JM, Myerson S, Selvanayagam JB and Neubauer S. The role of cardiovascular magnetic resonance imaging in heart failure. J Am Coll Cardiol. 2009;54:1407-24.

52 Senthilkumar A, Majmudar MD, Shenoy C, Kim HW and Kim RJ. Identifying the etiology: a systematic approach using delayed-enhancement cardiovascular magnetic resonance. Heart failure clinics. 2009;5:349-67, vi.

53 Abbasi SA, Ertel A, Shah RV, Dandekar V, Chung J, Bhat G, Desai AA, Kwong RY and Farzaneh-Far A. Impact of cardiovascular magnetic resonance on management and clinical decision-making in heart failure patients. Journal of cardiovascular magnetic resonance : official journal of the Society for Cardiovascular Magnetic Resonance. 2013;15:89.

54 Kim HW, Farzaneh-Far A and Kim RJ. Cardiovascular magnetic resonance in patients with myocardial infarction: current and emerging applications. J Am Coll Cardiol. 2009;55:1-16.

55 Kramer CM. Role of Cardiac MR Imaging in Cardiomyopathies. Journal of nuclear medicine : official publication, Society of Nuclear Medicine. 2015;56 Suppl 4:39S-45S.

56 Levy D, Garrison RJ, Savage DD, Kannel WB, Castelli WP. Prognostic implications of echocardiographically determined left ventricular mass in the Framingham Heart Study. The New England journal of medicine 1990;322:1561-6.

57 Marwick TH, Gillebert TC, Aurigemma G et al. Recommendations on the use of echocardiography in adult hypertension: a report from the European Association of Cardiovascular Imaging (EACVI) and the American Society of Echocardiography (ASE)dagger. European heart journal cardiovascular Imaging 2015;16:577-605.

58 Maceira AM, Mohiaddin RH. Cardiovascular magnetic resonance in systemic hypertension. Journal of cardiovascular magnetic resonance : official journal of the Society for Cardiovascular Magnetic Resonance 2012;14:28.

59 Rudolph A, Abdel-Aty H, Bohl S et al. Noninvasive detection of fibrosis applying contrast-enhanced cardiac magnetic resonance in different forms of left ventricular hypertrophy relation to remodeling. J Am Coll Cardiol 2009;53:284-91.

60 Germans T, Nijveldt R, Brouwer WP et al. The role of cardiac magnetic resonance imaging in differentiating the underlying causes of left ventricular hypertrophy. Netherlands heart journal : monthly journal of the Netherlands Society of Cardiology and the Netherlands Heart Foundation 2010;18:135-43.

61 Kwong RY, Farzaneh-Far A. Measuring myocardial scar by CMR. JACC Cardiovascular imaging 2011;4:157-60.

62 Parsai C, O'Hanlon R, Prasad SK, Mohiaddin RH. Diagnostic and prognostic value of cardiovascular magnetic resonance in non-ischaemic cardiomyopathies. Journal of cardiovascular magnetic resonance : official journal of the Society for Cardiovascular Magnetic Resonance 2012;14:54.

63 Krittayaphong R, Boonyasirinant T, Chaithiraphan V et al. Prognostic value of late gadolinium enhancement in hypertensive patients with known or suspected coronary artery disease. The international journal of cardiovascular imaging 2010;26 Suppl 1:123-31.

64 Andersen K, Hennersdorf M, Cohnen M, Blondin D, Modder U, Poll LW. Myocardial delayed contrast enhancement in patients with arterial hypertension: initial results of cardiac MRI. Eur J Radiol 2009;71:75-81.

65 Rodrigues JC, Amadu AM, Dastidar AG et al. Comprehensive characterisation of hypertensive heart disease left ventricular phenotypes. Heart 2016;102:1671-9.